Study of the reaction $\bar{p}n \to \pi^+\pi^-\pi^-$ between 1.09 and 1.43 GeV/c

J. M. Mountz,* Z. Ming Ma, and P. Zemany†
Department of Physics, Michigan State University, East Lansing, Michigan 48824
(Received 26 May 1977; revised manuscript received 11 August 1977)

We have analyzed the reaction $\bar{p}n \to \pi^+\pi^-\pi^-$ in a deuterium bubble-chamber experiment for incident antiproton momenta between 1.09 and 1.43 GeV/c. Data are analyzed in terms of the Veneziano model. The magnitudes of the spin-parity functions are determined independently in an analysis of the spin-state composition of the $\bar{p}n$ system. The amount of each spin-dependent Veneziano amplitude is contrained to these values in the construction of a Veneziano model. The model is found to be generally in good agreement with the data. This represents a more rigorous test of the Veneziano model than previously published works.

I. INTRODUCTION

One of the most successful models ever presented to explain high-energy scattering phenomenology is the Regge-pole model.[1,2] The model asserts that at high energies, i.e., when total c.m. energy is large, the scattering amplitude is dominated by particle exchange in the t channel. The asymptotic behavior for the Regge-pole amplitude is given[3] by

$$A(s,t) \sim g(t) s^{\alpha(t)}, \tag{1}$$

where the Mandelstam variables s and t are defined in the conventional manner.[4] On the other hand (except for K^+N interactions), low-energy meson-baryon scattering processes are dominated by resonance production.[5] These facts lead to entirely different mathematical parametrizations for low- and high-energy reactions.

An elegant dual model[6] was proposed by Veneziano which offers a simple description of the scattering data for low energy as well as asymptotic regions of s. Its original form exhibits Regge behavior and is explicitly crossing symmetric:

$$\begin{aligned} A(s,t,u) = \frac{\beta}{\pi} [&B(1-\alpha(t), 1-\alpha(s)) \\ &+ B(1-\alpha(t), 1-\alpha(u)) \\ &+ B(1-\alpha(s), 1-\alpha(u))] \end{aligned} \tag{2}$$

where B is the Euler beta function and is defined by

$$B(x,y) = \frac{\Gamma(x)\Gamma(y)}{\Gamma(x+y)}, \tag{3}$$

and β is a constant. The function $\alpha(s)$ is the Regge trajectory in the s channel and $\Gamma(x)$ is the Γ function. It is evident by examining Eq. (3) that the poles of the Γ function at $0, -1, -2, \ldots, -N$ lie on the real part of the s axis if $\alpha(s)$ is real. By allowing $\alpha(s)$ to be imaginary, not only may one move these poles to an acceptable unphysical region, but one will also give appropriate widths to the direct-channel resonances.

The modified trajectory for a 2π system can be written as

$$\alpha(s) = A + Bs + iC(s - 4M^2)^{1/2}, \tag{4}$$

where A and B describe a linearly rising trajectory, and C depends on the width of the s-channel resonances. The quantity M is the mass of the pion.

Anninos *et al.*[7] studied the reactions $\bar{p}n \to \pi^+\pi^-\pi^-$ at rest in a high-statistics experiment. In addition to the apparent production of ρ^0 and f^0, the authors noted the presence of a hole near the center of the Dalitz plot and the lack of events in the region where one of the $\pi^+\pi^-$ masses is small and the other is large.

Lovelace first applied the Veneziano model to these data[8] to explain the structures observed in the Dalitz plot, assuming that the initial spin-parity state is 0^-.

Bettini *et al.*[9] examined the reaction $\bar{p}n \to \pi^+\pi^-\pi^-$ for laboratory momenta between 1.0 and 1.6 GeV/c and compared their data with the predictions of the Veneziano model. A phenomenological approach was taken with regard to the spin-parity state of the $\bar{p}n$ system. They found that the Veneziano model was in good agreement with their data if the spin-parity of the $\bar{p}n$ system was assumed to be entirely 2^+. However, contributions by other states could not be ruled out. An alternative interpretation of the data was proposed by Odorico.[10] In a dual model, the structures in the Dalitz plot are attributed to resonance formation.

In this analysis, the reaction

$$\bar{p}n \to \pi^+\pi^-\pi^- \tag{5}$$

was analyzed using the Veneziano model. It should be noted that without prior knowledge or assumption of the spin structure, one is faced with the task of choosing from among an enormous number

of different combinations of states. Without infinite statistics, it may be purely accidental that a certain combination of states should fit the data well. In this analysis, the amount of each spin-parity state is determined by an examination of the angular distributions of the resonance intermediate states. The results are then used to constrain the magnitude of the corresponding Veneziano amplitudes.

II. THE DATA SAMPLE

The data for this analysis consist of 1914 events at 1.09, 1.19, 1.31, and 1.43 GeV/c obtained from an exposure in the Brookhaven National Laboratory 31-in. deuterium bubble chamber. Details for this experiment will be published elsewhere.[11] Figure 1(A) shows the Dalitz plot for the $\pi^+\pi^-$ system. Its projection onto the invariant-mass-squared axis is given in Fig. 1(B). Here one observes an obvious abundant production of the ρ^0 and f^0 states. From a fit of the data to an incoherent sum of

$$\bar{p}n \to \rho^0\pi^-, \tag{6}$$

$$\bar{p}n \to f^0\pi^-, \tag{7}$$

$$\bar{p}n \to \pi^+\pi^-\pi^- \text{ (nonresonant)} \tag{8}$$

states, the fractional amounts of the above reactions are determined to be 0.290 ± 0.026, 0.464 ± 0.031, and 0.246 ± 0.044, respectively. The masses and widths are found to be 761 ± 7 and 165 ± 11 MeV for ρ^0 and 1278 ± 7 and 176 ± 13 MeV for f^0. The dominance by resonance production allows one to extract dynamic characteristics of either the $\rho^0\pi^-$ or $f^0\pi^-$ intermediate states. For ρ^0 production, events of invariant mass from 640 to 880 MeV are considered to be in the signal region. The control bands are from 540 to 640 MeV and from 880 to 980 MeV. Assuming that the angular distribution for the background events varies smoothly between the control bands and the signal band, one can obtain the angular distribution for the signal. This was done by normalizing the total number of events in the control bands to the background in the resonance band, and then subtracting the angular distribution of the control bands from the resonance band. Fig. 2(B) shows the angular distribution for reaction (6). The angle θ is defined as the c.m. scattering angle of the resonance particle with respect to the incident antiproton. For f^0 production the resonance produced events were taken from 1160 to 1400 MeV with control band cuts from 940 to 1140 MeV and from 1420 to 1520 MeV. Fig. 2(B) shows the angular distribution for reaction

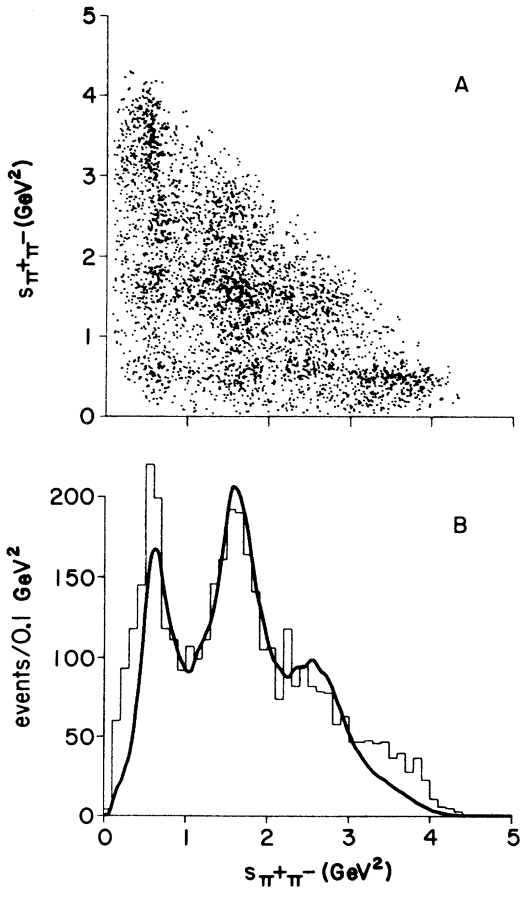

FIG. 1. (A) The Dalitz plot of $s(\pi^+\pi_1^-)$ vs $s(\pi^+\pi_2^-)$. (B) The projection onto the mass-squared axis. The prediction of the Veneziano model is shown as a smooth curve.

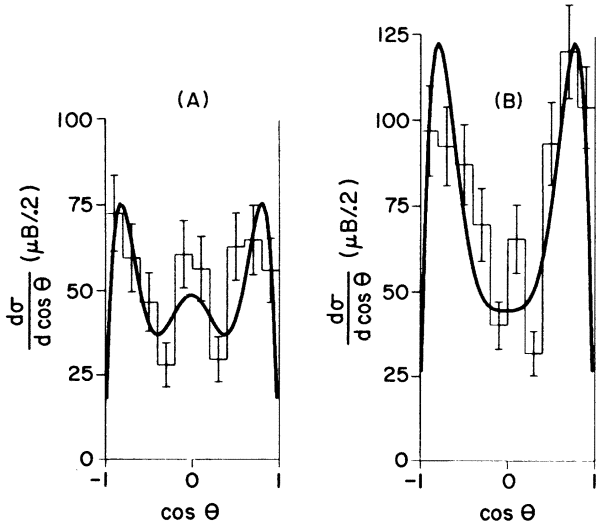

FIG. 2. Angular distributions for (A) ρ^0 production and (B) f^0 production. Details for background subtraction are discussed in the text.

(7), which was obtained using the same procedure discussed above. The numbers of resonance events in the signal regions were found to be 346 and 544 for the ρ^0 and f^0 meson, respectively. The angular distribution of the background was fairly flat and amounted to 0.42 and 0.41 of the events in the ρ^0 and f^0 signal regions, respectively.

III. SPIN DETERMINATION OF THE ANTIPROTON-NEUTRON SYSTEM

Consider the reaction $A+B \to C+D$. One can relate the helicity amplitudes to the differential cross section by[12]

$$\frac{d\sigma}{d\Omega} = \frac{1}{(2S_a+1)} \frac{1}{(2S_b+1)} \sum_{abcd} |f_{c,d,a,b}|^2 , \tag{9}$$

where the scattering amplitude is written as

$$f_{\lambda_c,\lambda_d,\lambda_a,\lambda_b}(s,\theta) = \frac{1}{q} \sum_J (2J+1) T^J_{\lambda_c,\lambda_d,\lambda_a,\lambda_b}(s) \times d^J_{\lambda,\mu}(\theta) , \tag{10}$$

and $T^J_{\lambda_c,\lambda_d,\lambda_a,\lambda_b}(s)$ is the transition amplitude. The function $d^J_{\lambda,\mu}(\theta)$ is a single-variable rotation matrix.[13]

The variables s and q represent the energy squared and initial momentum in the c.m. system, respectively. The symbol J is the total spin of the $\bar{p}n$ system. The helicities of particles C, D, A, and B are written as λ_c, λ_d, λ_a, and λ_b, respectively. The relative helicities λ and μ are defined as $\lambda_a - \lambda_b$ and $\lambda_c - \lambda_d$. Parity conservation requires that the amplitudes satisfy

$$T^J_{-\lambda_c,-\lambda_d,-\lambda_a,-\lambda_b} = \eta_a\eta_b\eta_c\eta_d(-1)^{S_c+S_d-S_a-S_b} \times T^J_{\lambda_c,\lambda_d,\lambda_a,\lambda_b} , \tag{11}$$

where $\eta_a, \eta_b, \eta_c, \eta_d$ are the intrinsic parities of the particles and S_c, S_d, S_a, S_b are their spins.

Consider particle C to be either the ρ^0 or f^0 meson, and particle D to be the π^- meson, one knows that the spin and parities of these particles are 1^-, 2^+, and 0^-, respectively. One further knows that the antiproton and neutron have spin $\frac{1}{2}$ and opposite intrinsic parity. This means $\eta_a\eta_b = -1$, and Eq. (11) becomes

$$T^J_{-\lambda_c,-\lambda_a,-\lambda_b} = -T^J_{\lambda_c,\lambda_a,\lambda_b}$$

for both the ρ^0 and f^0 mesons. The helicities which must be considered for the antiproton and neutron are $\pm\frac{1}{2}$. The ρ^0 may be $\pm1, 0$ and for the f^0 one has $\pm2, \pm1, 0$. The factor $\sum_{abcd}|f_{cdab}|^2$ for the ρ^0 meson can be explicitly written as follows, where the unconventional definition $D^J_{\lambda,\mu} = [(2J+1)/q]d^J_{\lambda,\mu}(\theta)$ is utilized:

$$\begin{aligned}\sum_{abcd}|f_{cdab}|^2 = {} & \left(\sum_J T^J_{1,1/2,-1/2}D^J_{1,1}\right)^2 + \left(\sum_J T^J_{1,1/2,1/2}D^J_{0,1}\right)^2 + \left(\sum_J T^J_{1,-1/2,1/2}D^J_{-1,1}\right)^2 + \left(\sum_J T^J_{1,-1/2,-1/2}D^J_{0,1}\right)^2 \\ & + \left(\sum_J T^J_{0,1/2,-1/2}D^J_{1,0}\right)^2 + \left(\sum_J T^J_{0,1/2,1/2}D^J_{0,0}\right)^2 + \left(\sum_J T^J_{0,-1/2,1/2}D^J_{-1,0}\right)^2 \\ & + \left(\sum_J T^J_{0,-1/2,-1/2}D^J_{0,0}\right)^2 + \left(\sum_J T^J_{-1,1/2,-1/2}D^J_{1,-1}\right)^2 + \left(\sum_J T^J_{-1,1/2,1/2}D^J_{0,-1}\right)^2 \\ & + \left(\sum_J T^J_{-1,-1/2,1/2}D^J_{-1,-1}\right)^2 + \left(\sum_J T^J_{-1,-1/2,-1/2}D^J_{0,-1}\right)^2 . \end{aligned} \tag{12}$$

The symmetry relations for $d^J_{\lambda,\mu}(\theta)$ are

$$d^J_{\lambda,\mu}(\theta) = d^J_{-\mu,-\lambda}(\theta) = (-1)^{\lambda-\mu}d^J_{\mu,\lambda}(\theta) .$$

This means

$$D^J_{1,1} = D^J_{-1,-1} , \quad D^J_{1,-1} = D^J_{-1,1} , \quad \text{and} \quad D^J_{0,1} = D^J_{-1,0} = -D^J_{0,-1} = -D^J_{1,0} .$$

Using the symmetry relations for $T^J_{\lambda_c,\lambda_a,\lambda_b}$ and $D^J_{\lambda,\mu}$, the right-hand side of Eq. (12) becomes

$$\begin{aligned} 2\times\Bigg[& \left(\sum_J T^J_{1,1/2,-1/2}D^J_{1,1}\right)^2 + \left(\sum_J T^J_{-1,1/2,-1/2}D^J_{1,-1}\right)^2 + \left(\sum_J T^J_{0,1/2,1/2}D^J_{0,0}\right)^2 \\ & + \left(\sum_J T^J_{1,1/2,1/2}D^J_{0,1}\right)^2 + \left(\sum_J T^J_{1,-1/2,-1/2}D^J_{0,1}\right)^2 + \left(\sum_J T^J_{0,-1/2,1/2}D^J_{0,1}\right)^2\Bigg] . \end{aligned} \tag{13}$$

The last three terms of Eq. (13) have the same angular distribution, even though they correspond to different helicity amplitudes. Because the interest here is the initial-spin state, and because the unique separation of the last three terms is impossible, Eq. (13) is rewritten as

$$2\times\left[\left(\sum_J T^J_{1,1/2,-1/2}D^J_{1,1}\right)^2+\left(\sum_J T^J_{-1,1/2,-1/2}D^J_{1,-1}\right)^2+\left(\sum_J T^J_{0,1/2,1/2}D^J_{0,0}\right)^2+\left(\sum_J R^J D^J_{0,1}\right)^2\right], \tag{14}$$

where $(\sum_J R^J D^J_{0,1})^2$ has been written in place of the last three terms. One finally obtains the expression for the angular differential cross section of the ρ^0 meson as

$$\pi\left[\left(\sum_J T^J_{1,1/2,-1/2}D^J_{1,1}\right)^2+\left(\sum_J T^J_{-1,1/2,-1/2}D^J_{1,-1}\right)^2+\left(\sum_J T^J_{0,1/2,1/2}D^J_{0,0}\right)^2+\left(\sum_J R^J D^J_{0,1}\right)^2\right]. \tag{15}$$

For the f^0 meson the additional helicity states of ± 2 must be considered. This leads to an expression involving all the terms above, plus the additional ones

$$\pi\left[\left(\sum_J T^J_{2,1/2,-1/2}D^J_{-1,-2}\right)^2+\left(\sum_J T^J_{2,-1/2,1/2}D^J_{1,-2}\right)^2+\left(\sum_J F^J D^J_{0,2}\right)^2\right], \tag{16}$$

where

$$\left(\sum_J F^J D^J_{0,2}\right)^2=\left(\sum_J T^J_{2,1/2,1/2}D^J_{0,2}\right)^2+\left(\sum_J T^J_{2,-1/2,-1/2}D^J_{0,2}\right)^2. \tag{17}$$

The distributions were fitted to angular functions for J values up to and including 4. A typical term in the fit involving the complex transition matrix elements $T^J_{\lambda_c,\lambda_a,\lambda_b}$ would appear as

$$\pi\sum_{JJ'} T^J_{\lambda_c,\lambda_a,\lambda_b}T^{J'*}_{\lambda_c,\lambda_a,\lambda_b}D^J_{(\lambda_a-\lambda_b),\lambda_c}D^{J'}_{(\lambda_a-\lambda_b),\lambda_c}. \tag{18}$$

The transition amplitudes were normalized according to

$$\frac{d\sigma}{d(\cos\theta)}=\sigma_T\sum_{\lambda_c\lambda_a\lambda_b}\sum_{JJ'}\left(\frac{(2J+1)}{2}\right)^{1/2}\left(\frac{(2J'+1)}{2}\right)^{1/2}T^J_{\lambda_c,\lambda_a,\lambda_b}T^{J'*}_{\lambda_c,\lambda_a,\lambda_b}d^J_{\lambda,\mu}d^{J'}_{\lambda,\mu}, \tag{19}$$

and the usual normalization

$$\int d^J_{\lambda,\mu}(\cos\theta)d^{J'}_{\lambda,\mu}(\cos\theta)d(\cos\theta)=\delta_{JJ'}\frac{2}{(2J+1)} \tag{20}$$

was maintained.

The least-squares method was used to fit Eq. (15) to the ρ^0 angular distribution for all combinations of total spin and helicity. The f^0 angular distribution is fitted independently to a sum of the terms in Eqs. (15) and (16). Considering J values greater than 3 did not improve the χ^2 per degree of freedom. In the final fit, only those terms with a contribution inconsistent with being zero are kept. The resultant terms are found to be an incoherent sum of the helicity amplitudes represented by R^J and F^J. The results are given in Table I and the fitted curves are shown as solid lines in Figs. 2(A) and 2(B) for ρ^0 and f^0 production processes, respectively. The final χ^2 per degree of freedom are 2.0 and 3.4 for the ρ^0 and f^0 angular distributions, respectively.

TABLE I. Spin-state composition of the $\bar{p}n$ system.

Total spin	Amount of ρ (percent)	Amount of f (percent)
$J=1$	0.31 ± 0.07	0.16 ± 0.05
$J=2$	0.28 ± 0.08	0.52 ± 0.06
$J=3$	0.33 ± 0.07	0.24 ± 0.05
Total	0.91 ± 0.22	0.92 ± 0.16

IV. THE SPIN-DEPENDENT VENEZIANO MODEL

The problem of constructing an amplitude describing the decay of a state of given spin, parity, and isospin into three pions has been investigated by Zemach[14] and Goebel *et al.*[15] Goebel studied the specific problem of constructing Veneziano amplitudes for definite spin-parity states. In Goebel's derivation a full amplitude is obtained by multiplying a spin factor times a scalar Veneziano am-

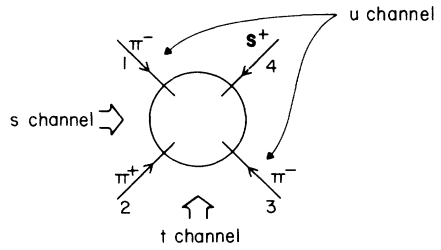

FIG. 3. Diagram for the scattering process $\pi^-\pi^+ \to \pi^+ s^-$.

plitude. The spin factor consists of products involving the momenta vectors of the final-state particles. The scalar Veneziano amplitudes differ for different spin-parity states because the full amplitude is required to exhibit Regge behavior.

In order to better understand how the Veneziano model will be related to the reaction $\bar{p}n \to \pi^+\pi^-\pi^-$ discussed here, one is led to consider the scattering process $\pi^-\pi^+ \to \pi^+ s^-$ where particles s^- with spin S represent the $\bar{p}n$ system. This process is shown in Fig. 3, with all four particles taken as incoming.

In reference to Fig. 3, the Mandelstam variables are defined as

$$s = s_{12} = -(P_1 + P_2)^2 , \tag{21}$$

$$t = s_{23} = -(P_2 + P_3)^2 , \tag{22}$$

and

$$u = s_{13} = -(P_1 + P_3)^2 . \tag{23}$$

The dual nature of the Veneziano model requires one to consider known resonances in all three channels since resonant effects in one channel must be identical in the duality sense to particle exchange in the crossed channel. One can see that both the s and t channels are identical and may have resonances, while the u channel with isospin $|I, I_z\rangle = |2, -2\rangle$ cannot.

If the $\bar{p}n$ system has the natural spin-parity quantum numbers ($S^P = 1^-, 2^+, 3^-, \ldots$), one may write the full amplitude for the above-mentioned scattering process[15] as

$$A(s_{12}, s_{23}) = \text{const} \times [\epsilon_{\mu\alpha\beta\gamma} P_{1_\alpha} P_{2_\beta} P_{3_\gamma} S_\mu \ldots \times (P_3)^L (P_1)^M V(s_{12}, s_{23}) + (1 \leftrightarrow 3)], \tag{24}$$

where $S_\mu \ldots$ is the polarization tensor of the $\bar{p}n$ system. $\epsilon_{\mu\alpha\beta\gamma} = 0$ if any indices are equal, -1 for odd permutations of the indices, and $+1$ for even permutations of the indices. The product $S_\mu \ldots (P_3)^L (P_1)^M$ is understood to mean the contraction of the polarization tensor $S_\mu \ldots$ with L factors of P_3 and M factors of P_1. The indices L and M satisfy the relationship $L + M = S - 1$. The contracted product has vector qualities and the amplitude is a scalar. The notation $(1 \leftrightarrow 3)$ will mean to symmetrize the previous term by interchanging particles 1 and 3. $V(s_{12}, s_{23})$ is the appropriate Veneziano scalar amplitude for the particular spin-parity state being considered. The requirement for $A(s_{12}, s_{23})$ to exhibit Regge behavior allows the Veneziano amplitude discussed here to have the form

$$V(s_{12}, s_{23}) = \frac{\Gamma(S - L - \alpha(s_{12}))\Gamma(S - M - \alpha(s_{23}))}{\Gamma(S + 1 - \alpha(s_{12}) - \alpha(s_{23}))} . \tag{25}$$

If the $\bar{p}n$ system has unnatural spin-parity quantum numbers ($S^P = 0^-, 1^+, 2^-, \ldots$) the amplitude may similarly be written

$$A(s_{12}, s_{23}) = \text{const} \times S_\mu \ldots (P_3)^L (P_1)^M V(s_{12}, s_{23}) + (1 \leftrightarrow 3) , \tag{26}$$

where now $S = L + M$ is required. The requirement of Regge behavior dictates that the form of the Veneziano amplitude be

$$V(s_{12}, s_{23}) = \frac{\Gamma(m - \alpha(s_{12}))\Gamma(n - \alpha(s_{23}))}{\Gamma(m + n - p - \alpha(s_{12}) - \alpha(s_{23}))} , \tag{27}$$

where $m \geq M + p$, $n \geq L + p$, and $p = \text{integer} \geq 0$. Further, one must have $m \geq 1$ and $n \geq 1$ to avoid the poles at $\alpha(s_{ij}) = 0$.

All spin-parity states up to a spin of 4 are considered with the exception of 0^+, 1^-, and 3^-. For a three-pion system with arbitrary total angular momentum J, one may write the parity as $P = \eta^3(-1)^L(-1)^l$ where l is the relative orbital angular momentum of the $\pi^+\pi^-$ system, and L is the orbital angular momentum of the third pion with respect to that system. Here $\eta = -1$ is the intrinsic parity of the pion. If $J = 0$, then $L = l$ and $P = \eta^3 = -1$; therefore 0^+ is forbidden.

Now consider the natural-parity states $J^P = 1^-, 2^+, 3^-, \ldots$ of a fermion-antifermion system of total spin angular momentum S and relative orbital angular momentum l. The parity (P), G parity (G), and charge-conjugation operator (C) are defined as $-(-1)^l$, $(-1)^{l+S+I}$, and $(-1)^{l+S}$, respectively, where I is the isotopic spin. Since there are no singlet states, one has $S = 1$ and $C = P$. The isotopic spin of the $\bar{p}n$ system is 1; therefore $G = C(-1)^1 = -P$. For a system of N pions, one has $G = (-1)^N$ or here $G = (-1)^3 = -1$. Since $G = -P$, P must be positive; therefore the states $1^-, 3^-, \ldots$ are forbidden.

The function α is taken as the ρ-f exchange-degenerate trajectory. Only Veneziano terms with leading asymptotic behavior are used. The amplitude for each spin-parity state is given by

$$0^-:\ A = \frac{\Gamma(1-\alpha(s_{12}))\Gamma(1-\alpha(s_{23}))}{\Gamma(1-\alpha(s_{12})-\alpha(s_{23}))}\,, \tag{28a}$$

$$1^+:\ A^i = P_1^i \frac{\Gamma(1-\alpha(s_{12}))\Gamma(2-\alpha(s_{23}))}{\Gamma(2-\alpha(s_{12})-\alpha(s_{23}))} + p_3^i \frac{\Gamma(1-\alpha(s_{23}))\Gamma(2-\alpha(s_{12}))}{\Gamma(2-\alpha(s_{12})-\alpha(s_{23}))}\,, \tag{28b}$$

$$2^-:\ A^{ij} = [(P_{3i}P_{1j}+P_{1i}P_{3j}) - \tfrac{1}{3}\delta_{ij}(P_{3i}P_{1j}+P_{1i}P_{3j})] \frac{\Gamma(1-\alpha(s_{12}))\Gamma(1-\alpha(s_{23}))}{\Gamma(2-\alpha(s_{12})-\alpha(s_{23}))}\,, \tag{28c}$$

$$\begin{aligned} 2^+:\ A^{ij} = {} & [(\vec{P}_1\times\vec{P}_3)^i P_3^j + (\vec{P}_1\times\vec{P}_3)^j P_3^i] \frac{\Gamma(1-\alpha(s_{12}))\Gamma(2-\alpha(s_{23}))}{\Gamma(3-\alpha(s_{12})-\alpha(s_{23}))} \\ & + [(\vec{P}_3\times\vec{P}_1)^i P_1^j + (\vec{P}_3\times\vec{P}_1)^j P_1^i] \frac{\Gamma(1-\alpha(s_{23}))\Gamma(2-\alpha(s_{12}))}{\Gamma(3-\alpha(s_{12})-\alpha(s_{23}))}\,, \end{aligned} \tag{28d}$$

$$\begin{aligned} 3^+:\ A^{ijk} = {} & \{[P_3^i P_3^j P_1^k + P_3^k P_3^i P_1^j + P_3^j P_3^k P_1^i] - \tfrac{1}{5}\delta_{ij}(|\vec{P}_3|^2 P_1^k + 2P_3^k \vec{P}_1\cdot\vec{P}_3) \\ & - \tfrac{1}{5}\delta_{ik}[|\vec{P}_3|^2 P_1^j + 2(\vec{P}_1\cdot\vec{P}_3)P_3^j] - \tfrac{1}{5}\delta_{jk}[|\vec{P}_3|^2 P_1^i + 2(\vec{P}_1\cdot\vec{P}_3)P_3^i]\} \\ & \times \frac{\Gamma(1-\alpha(s_{12}))\Gamma(2-\alpha(s_{23}))}{\Gamma(3-\alpha(s_{12})-\alpha(s_{23}))} + (1 \longleftrightarrow 3)\,. \end{aligned} \tag{28e}$$

V. ANALYSIS

The Dalitz plot is especially well suited for comparisons with the Veneziano model since the scalar amplitude has only two independent variables aside from an overall scale factor. The Dalitz plot is shown in Fig. 1(A). Each event is plotted twice for the two $\pi^+\pi^-$ combinations. The data sample consists of the 1914 events (3828 points on the Dalitz plot) with incident momentum from 1.09 to 1.43 GeV/c. Fig. 1(B) shows the Dalitz-plot projection onto the invariant-mass-squared axis. One observes strong ρ^0 and f^0 resonance bands at 0.58 and 1.64 GeV^2, respectively. The minimum density areas, in between the resonance bands, on the Dalitz plot are also very evident.

The values of A and B in Eq. (4) were obtained by simultaneously solving

$$\alpha(s=M_\rho^2) = 1 = A + B(M_\rho^2) \tag{29}$$

and

$$\alpha(s=M_f^2) = 2 = A + B(M_f^2)\,, \tag{30}$$

where M_ρ and M_f are taken to be 761 and 1278 MeV and were obtained by fitting the $\pi^+\pi^-$ invariant-mass distribution to Breit-Wigner resonance forms as discussed before. The parameter C in Eq. (4) was determined by requiring that the Veneziano model give the correct width to the observed ρ^0 meson. Table II lists A, B, and C. The values obtained here are comparable to those used by Lovelace, Bettini, and the normally accepted values[16] for the ρ trajectory.

The total transition matrix element squared, $|T|^2$, is expressed in terms of the Dalitz-plot parameters as

$$|T|^2 = \sum_{J^P} a^{J^P} |T^{J^P}(s_{12}, s_{23})|^2\,, \tag{31}$$

where $|T^{J^P}(s_{12}, s_{23})|^2$ is the square of the transition matrix elements given in Eq. (28). No interference terms are necessary since decay amplitudes from states of definite spin and parity are considered here. The variable a^{J^P} is the percentage of each contributing spin-parity state.

The overall normalization to the data is the only free parameter in this fit. The other four parameters, involving the relative amounts of the spin-dependent Veneziano amplitudes for the 1^+, 2^-, 2^+, and 3^+ states were constrained to be within 2 standard deviations of the values given in Table I.

The fit was performed by comparing the Dalitz-plot density in grid sizes of 0.5×0.5 GeV^4. Approximately 60 000 events were generated by a Monte Carlo routine.[17] These events were further weighted according to the actual number of events present at each momentum and to the magnitude of the square of the transition matrix element. Since the parity of the spin-2 state could not be determined in Sec. III, contributions from both the 2^+ and 2^- states were assumed possible. Fitted re-

TABLE II. A comparison of the ρ^0 trajectory parameters.

	This experiment	Lovelace	Bettini *et al.*	Accepted value
A	0.46 ±0.03	0.483	0.65	0.48
B	0.94 ±0.01	0.885	0.84	0.90
C	0.250 ±0.003	0.28	0.26	···

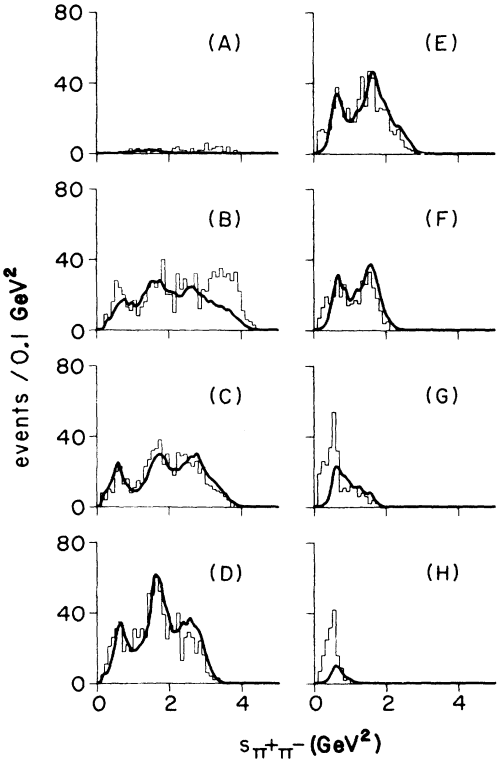

FIG. 4. The comparison of the Veneziano-model fit to the data for specific $\pi^+\pi^-$ mass-squared slices. (A) 0.0 to 0.2 GeV^2, (B) 0.2 to 0.8 GeV^2, (C) 0.8 to 1.4 GeV^2, (D) 1.4 to 1.9 GeV^2, (E) 1.9 to 2.5 GeV^2, (F) 2.5 to 3.0 GeV^2, (G) 3.0 to 3.6 GeV^2, (H) 3.6 to 5.0 GeV^2.

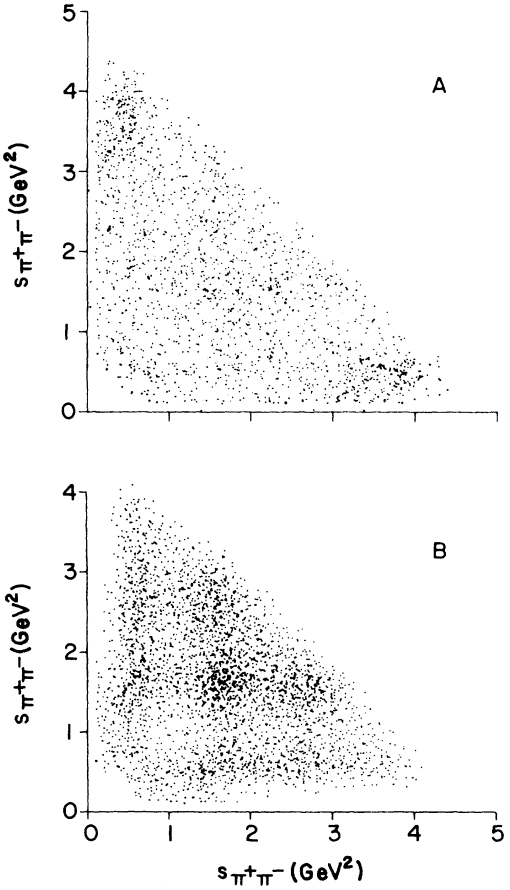

FIG. 5. Dalitz plot of the Veneziano-model fit. (A) The absolute deviation between the model and the data. (B) The model prediction.

sults are given in Fig. 1 as a smooth curve. The final values for the percent of each spin-parity used in the construction of the total Veneziano amplitude were 0.16, 0.001, 0.68, and 0.16 for the 1^+, 2^-, 2^+, and 3^+ states, respectively. Fig. 4 shows comparisons with the data for specific slices of the $\pi^+\pi^-$ mass squared. Overall, one observes agreement between the data and the model. The quality of the agreement between the data and the model here is comparable to that obtained by Bettini *et al.* The absolute magnitude of the difference between the data and the model prediction on the Dalitz plot is shown in Fig. 5(A). The areas where agreement is somewhat poor are at places where s_{12} is large and s_{23} is small and vice versa. This is similar to that observed by Bettini *et al.* Fig. 5(B) shows a Dalitz plot predicted by the model.

VI. SUMMARY AND CONCLUSIONS

The Dalitz plot for the invariant mass squared of the $\pi^+\pi^-$ system shows strong ρ^0 and f^0 bands. The minimum-density areas between the bands are also observed. The predictions of the Veneziano model were compared to data for incident momenta 1.09, 1.19, 1.31, and 1.43 GeV/c.

In this analysis, the scattering amplitudes are constructed specifically as products of the tensor spin-parity functions times the respective scalar Veneziano amplitudes. The magnitudes of the spin-parity functions are determined independently in an analysis of the spin-state composition of the $\bar{p}n$ system. The predictions of the Veneziano model are found to be in agreement with the data. The ability of the model to follow the relative magnitudes of the ρ^0, f^0, and g^0 resonances in Figs. 4(B)–4(F) should be noted. The relative strength of the $\pi^+\pi^-$ resonance bands depends critically on the spin-parity of the amplitudes. Since the $\bar{p}n$ spin-state composition is determined independently in this analysis, this analysis represents a more rigorous test of the Veneziano model.

ACKNOWLEDGMENT

We would like to thank the Brookhaven 31-in. bubble chamber crew and the AGS staff for a smooth run. The conscientious effort of the scanning and measuring staff at Michigan State University is gratefully acknowledged. This work was supported in part by the National Science Foundation.

---

*Now at Department of Biophysics, Michigan State University.
†Now at Department of Physics, University of Toronto, Canada M5S 1A7.

[1]T. Regge, Nuovo Cimento 14, 951 (1959).
[2]P. D. B. Collins, Physics Rep. 4C, 103 (1971).
[3]R. Omnès and M. Froissart, *Mandelstam Theory and Regge Poles* (Benjamin, New York, 1963), p. 102.
[4]William R. Frazer, *Elementary Particles* (Prentice-Hall, Englewood Cliffs, 1966), p. 16.
[5]Particle Data Group, Phys. Lett. 50B, 1 (1974).
[6]G. Veneziano, Nuovo Cimento 57A, 190 (1968).
[7]P. Anninos *et al.*, Phys. Rev. Lett. 20, 402 (1968).
[8]C. Lovelace, Phys. Lett. 28B, 264 (1968).
[9]A. Bettini *et al.*, Nuovo Cimento 1A, 333 (1971).
[10]R. Odorico, Phys. Lett. 33B, 489 (1970).
[11]J. M. Mountz, P. Zemany, and Z. Ming Ma (unpublished).
[12]J. D. Kimel, Florida State University report (unpublished).
[13]M. Jacob and G. C. Wick, Ann. Phys. (N.Y.) 7, 404 (1959).
[14]C. Zemach, Phys. Rev. 140, B97 (1965); 133, B1201 (1964)
[15]C. J. Goebel, Maurice L. Blackmon, and Kameshwar C. Wali, Phys. Rev. 182, 1487 (1969).
[16]J. D. Jackson, Rev. Mod. Phys. 42, 12 (1970).
[17]J. Friedman, Univ. of California, Berkeley, Group A Programming Note No. P-189 (unpublished).

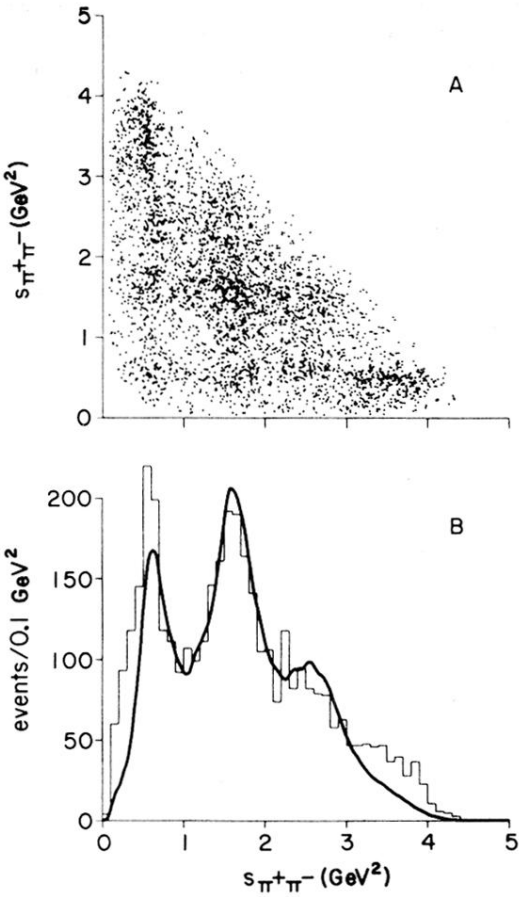

FIG. 1. (A) The Dalitz plot of $s(\pi^+\pi_1^-)$ vs $s(\pi^+\pi_2^-)$. (B) The projection onto the mass-squared axis. The prediction of the Veneziano model is shown as a smooth curve.

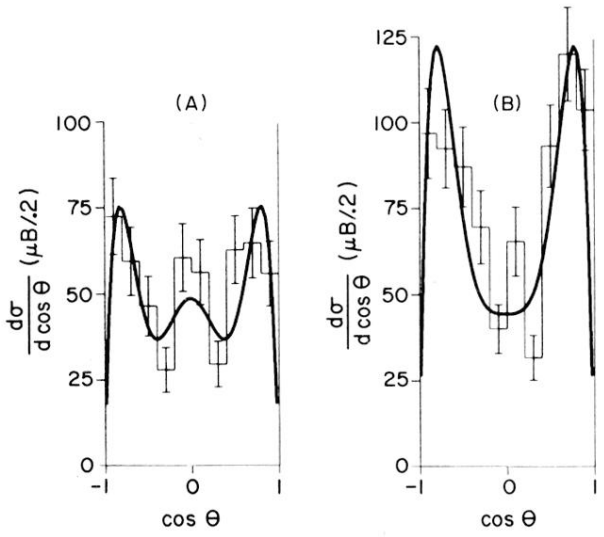

FIG. 2. Angular distributions for (A) ρ° production and (B) f° production. Details for background subtraction are discussed in the text.

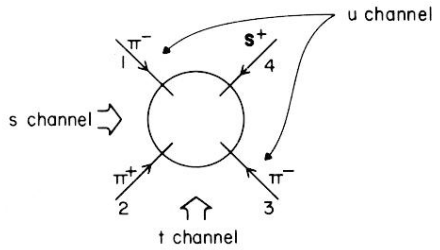

FIG. 3. Diagram for the scattering process $\pi^- \pi^+ \rightarrow \pi^+ s^-$.

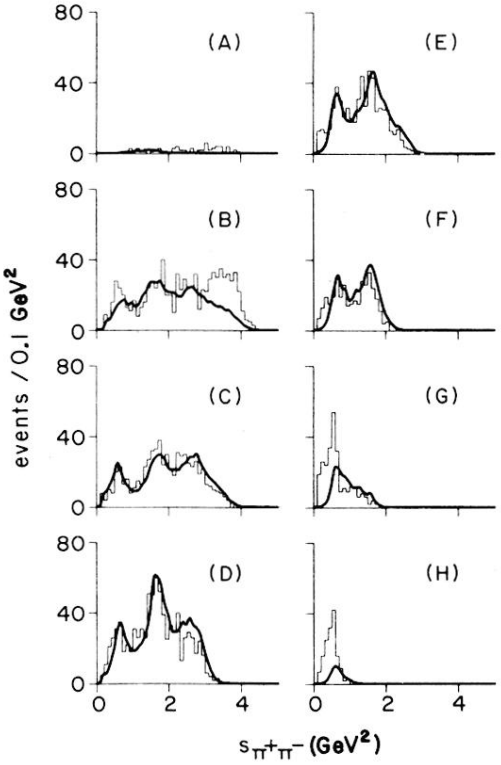

FIG. 4. The comparison of the Veneziano-model fit to the data for specific $\pi^+\pi^-$ mass-squared slices. (A) 0.0 to 0.2 GeV^2, (B) 0.2 to 0.8 GeV^2, (C) 0.8 to 1.4 GeV^2, (D) 1.4 to 1.9 GeV^2, (E) 1.9 to 2.5 GeV^2, (F) 2.5 to 3.0 GeV^2, (G) 3.0 to 3.6 GeV^2, (H) 3.6 to 5.0 GeV^2.

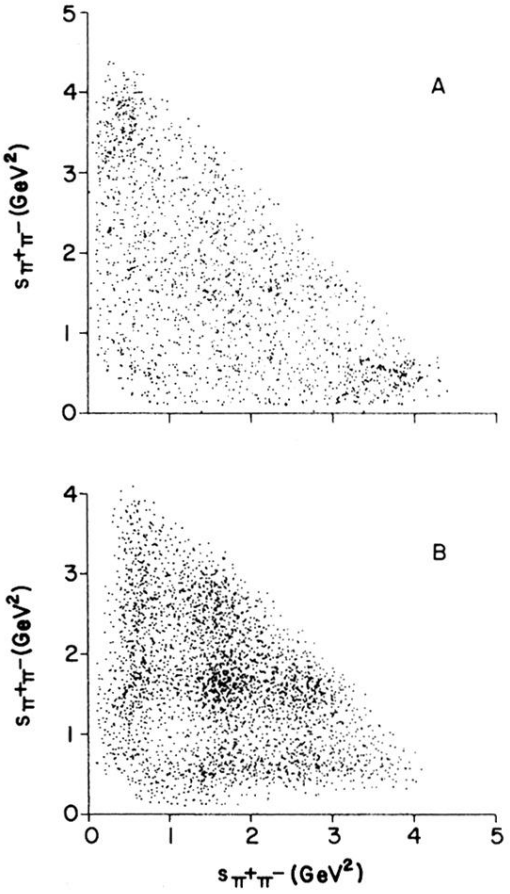

FIG. 5. Dalitz plot of the Veneziano-model fit. (A) The absolute deviation between the model and the data. (B) The model prediction.